Cancer Letters 380 (2016) 10–19

Contents lists available at ScienceDirect

Cancer Letters

journal homepage: www.elsevier.com/locate/canlet

Original Articles

Preclinical platform of retinoblastoma xenografts recapitulating human disease and molecular markers of dissemination

Guillem Pascual-Pasto [a,b], Nagore G. Olaciregui [a,b], Monica Vila-Ubach [a,b], Sonia Paco [a,b], Carles Monterrubio [a,b], Eva Rodriguez [a,b], Ursula Winter [c,d], Mireia Batalla-Vilacis [a], Jaume Catala [e], Hector Salvador [a,b], Andreu Parareda [a,b], Paula Schaiquevich [d,f], Mariona Suñol [c], Jaume Mora [a,b], Cinzia Lavarino [a,b], Carmen de Torres [a,b], Guillermo L. Chantada [a,b,f,g], Angel M. Carcaboso [a,b,*]

[a] *Developmental Tumor Biology Laboratory, Fundacio Sant Joan de Deu, Barcelona, Spain*
[b] *Department of Pediatric Hematology and Oncology, Hospital Sant Joan de Deu, Barcelona, Spain*
[c] *Pathology, Hospital Sant Joan de Deu, Barcelona, Spain*
[d] *Clinical Pharmacokinetics Unit, Hospital de Pediatria JP Garrahan, Buenos Aires, Argentina*
[e] *Ophthalmology, Hospital Sant Joan de Deu, Barcelona, Spain*
[f] *CONICET, Buenos Aires, Argentina*
[g] *Garrahan Research Institute, Hospital de Pediatria JP Garrahan, Buenos Aires, Argentina*

ARTICLE INFO

Article history:
Received 29 March 2016
Received in revised form 10 June 2016
Accepted 14 June 2016

Keywords:
Retinoblastoma
Xenograft
CRX
Metastasis
Tumor model

ABSTRACT

Translational research in retinoblastoma – a pediatric tumor that originates during the development of the retina – would be improved by the creation of new patient-derived models. Using tumor samples from enucleated eyes we established a new battery of preclinical models that grow *in vitro* in serum-free medium and *in vivo* in immunodeficient mice. To examine whether the new xenografts recapitulate human disease and disseminate from the retina to the central nervous system, we evaluated their histology and the presence of molecular markers of dissemination that are used in the clinical setting to detect extraocular metastases. We evaluated *GD2 synthase* and *CRX* as such markers and generated a Taqman real-time quantitative PCR method to measure *CRX* mRNA for rapid, sensitive and specific quantification of local and metastatic tumor burden. This approach was able to detect 1 human retinoblastoma cell in 100.000 mouse brain cells. Our research adds novel preclinical tools for the discovery of new retinoblastoma treatments for clinical translation.

© 2016 Elsevier Ireland Ltd. All rights reserved.

Introduction

Retinoblastoma is a rare solid tumor that arises during the normal development of the retina in 1 out of 17,000 children, due to mutations or inactivations in the *RB1* gene [1]. Intraocular retinoblastoma is highly curable by radical surgery (enucleation of the eye) but recent efforts have improved the eye salvage rates using intensive globe preserving therapies that include intra-ophthalmic artery and intravitreous delivery of chemotherapy [2–4]. However, some tumors progress after treatment into a chemoresistant phenotype and for such cases enucleation is necessary to prevent fatal extraocular dissemination of the disease to the central nervous system (CNS) [5].

Preclinical research in retinoblastoma requires *in vivo* models that reproduce the worst possible clinical scenario following aggressive eye-preservative therapies, i.e. chemoresistant tumors with metastatic properties. Such tumors can be obtained from enucleated eyes, processed in the laboratory, and transferred to mice to establish intraocular xenografts [6–8]. The pattern and extent of extraocular dissemination in the new retinoblastoma xenografts should be thoroughly studied to characterize each model and to detect the activity of novel therapies. Imaging techniques including magnetic resonance and bioluminescence help follow the extraocular disease at the macroscopic level, but they are technically challenging and not applicable in all the laboratories [9–11]. On the other hand, the follow up of microscopic disease in the preclinical setting has remained a challenge that requires experienced pathologists and extensive preparative work offering low sensitivity of detection [12].

In the clinical setting, minimal disseminated disease (MDD) in retinoblastoma is analyzed by morphological assessment of cerebrospinal fluid (CSF) and bone marrow (BM), but this technique provides low sensitivity and is limited to patients with regionally recurrent disease or symptoms of metastatic disease [13,14]. Therefore, gene expression analyses of CSF and BM by real-time

* Corresponding author. Tel.: +34 936009751; fax: +34 936009771.
E-mail address: amontero@fsjd.org (A.M. Carcaboso).

http://dx.doi.org/10.1016/j.canlet.2016.06.012
0304-3835/© 2016 Elsevier Ireland Ltd. All rights reserved.

quantitative PCR (RT-qPCR) have been proposed. Molecular MDD targets include GD2 synthase, the enzyme responsible for GD2 production [15]. GD2 is a disialoganglioside highly expressed in tumors derived from the neural crest and in some normal cells of the nervous system [16]. Another MDD target is the cone lineage specific marker cone-rod homeobox (CRX) transcription factor, which is uniformly expressed in retinoblastoma and in the normal retina, but not in other organs [7,17,18]. *GD2 synthase* and *CRX* mRNAs have been previously used as MDD markers in retinoblastoma patients [19–21]. However, it is unknown whether these markers could be also useful to detect MDD in animal models of human retinoblastoma or to correlate with the amount of viable tumor in a specific animal tissue.

Here we have established and characterized a series of new preclinical retinoblastoma models, most of them from patients bearing chemoresistant tumors. We have analyzed the expression of *GD2 synthase* and *CRX* in the new models and in the Y79 cell line. We propose a new, highly sensitive and 100% specific Taqman assay to quantify local burden of retinoblastoma and dissemination to distant sites.

Materials and methods

Procurement of tumor specimens and cell cultures

Tumor samples were obtained from enucleated eyes of retinoblastoma patients at Hospital Sant Joan de Deu (HSJD, Barcelona), under an IRB-approved protocol and informed consent. Specimens were collected from two possible sources: solid tumor tissue in the retina (retinoblastoma tumor; RBT) and tumor seeding in the vitreous humor (retinoblastoma vitreous seedings; RBVS). To obtain cell suspensions for cultures RBT specimens were disaggregated using a mixture of collagenase (400 UK/mL) and DNAse (5 mg/mL) (Sigma, St. Louis, MO) at 37 °C during 5 min; cells from RBVS samples were collected by centrifugation. After two washes with PBS, tumor cells were cultured as floating tumorspheres in neural stem cell medium (serum-free) as previously described [22]. We followed the same procedures as described by our group for pediatric glioma cell models (HSJD-DIPG-007, HSJD-DIPG-012 and HSJD-DIPG-013) established from biopsies of pediatric patients with diffuse intrinsic pontine glioma (DIPG) at HSJD [23].

Retinoblastoma cell line Y79 was obtained from Sigma and neuroblastoma cell lines SH-SY5Y, SK-N-LP, SK-N-JD and IMR-5 were obtained from the repository maintained at HSJD. Cell lines were cultured with RPMI high glucose medium supplemented with 10% FBS, 2 mM L-glutamine, penicillin (100 U/mL) and streptomycin (100 μg/mL) (Life Technologies, Grand Island, NY). All cultures were maintained at 37 °C in 5% CO_2 atmosphere.

Immunofluorescence (IF) and immunocytochemistry (IC)

To study the expression of GD2 and CRX in retinoblastoma cultures, tumorspheres were fixed with 4% paraformaldehyde for 20 min, permeated with 0.1% Triton X-100 (Sigma) and blocked for 30 min with 1% BSA (Sigma). For IF, primary GD2 antibody (554272, BD Biosciences, San Diego, CA) was incubated for 1 h at room temperature and DAPI (Sigma) was added for nuclear staining. For IC, endogenous peroxidases were inhibited with H_2O_2 for 20 min, primary CRX antibody (ab78662, Abcam, Cambridge, MA) was incubated for 1 h at room temperature and detection was performed with an anti-mouse/rabbit Poly-HRP IHC kit (Chemicon, Temecula, CA).

Immunoblotting

Retinoblastoma, pediatric glioma cell models, and mouse retinas were lysed with RIPA 1× buffer (50 mM Tris, 150 mM NaCl, 0.1% SDS, 0.5% Na deoxycholate, and 1% NP40; Sigma) and Complete Protease Inhibitor Cocktail Tablets (Roche, Indianapolis, IN) and whole protein extracts quantified with microBCA kit (Pierce, Rockford, IL). Samples (25 μg protein) were separated by electrophoresis in 12% polyacrylamide gels and transferred to nitrocellulose membranes (Invitrogen). Antibodies used were CRX (1:1000) and α-tubulin (T6199; 1:30000; Sigma). Western blot detection was performed with near-infrared labeled secondary antibodies (Odyssey CLx, LI-COR Inc, Bad Homburg, Germany).

Chromosomal microarray analysis

To compare the genetics of the original patient tumors and the established cell models we characterized the overall genomic aberrations in whole genome. Genomic DNA was obtained from retinoblastoma biopsies and paired cell cultures. Whole-genome analysis was performed using a high-density array (GeneChip™ HD CytoScan Array, Affymetrix, Santa Clara, CA, USA) that includes more than 2.6 million copy number variation markers (over 740,000 single-nucleotide polymorphism markers and more than 1.9 million nonpolymorphic markers). Total DNA (250 ng) for each sample was digested, ligated, PCR amplified and purified, fragmented, biotin-labeled, and hybridized according to manufacturer's protocols. CEL files obtained by scanning the arrays were analyzed using the Chromosome Analysis Suite software (Affymetrix). Gains and losses that affected a minimum of 50 and 25 markers, respectively, in a 100 kb length were considered.

Orthotopic retinoblastoma xenografts

Animal experiments were carried out in accordance with institutional and European guidelines (EU Directive 2010/63/EU) and complied with the ARRIVE guidelines [24]. Human retinoblastoma cells from seven newly established primary models and Y79 model were injected into the posterior segment of the eyes of 4–6 week old female athymic nude mice (Envigo, Barcelona, Spain). Animals (6–7 per cell model) were anesthetized with 100 mg/kg ketamine and 10 mg/kg xylazine and immobilized in a stereotaxic apparatus (Stoelting, Wood Dale, IL). With the help of a stereomicroscope (M80, Leica Microsystems, Barcelona, Spain) a small incision was performed in the corneal limbus with a 27 G needle. Then, 2×10^5 cells suspended in 2 μL matrigel (BD Biosciences) were introduced through the incision, at a 2 mm depth into the posterior segment of the eye with a dull 33 G needle attached to a 5 μL syringe (Hamilton, Bonaduz, Switzerland), using a stereotaxic arm. Animals recovered and intraocular tumors developed until invading the posterior and anterior chambers of the ocular globes causing proptosis. At that time eyes were considered to reach the experimental endpoint and were enucleated under general anesthesia. When both eyes achieved the endpoint status, mice were anesthetized to collect CSF from the cisterna magna, as previously described [25], and sacrificed. To study the histology of the tumors in the eyes and the dissemination to the CNS, tissues from at least one animal in each group were fixed in 4% PFA and embedded in paraffin.

To perform MDD analyses by RT-qPCR in selected tissues, the intraocular content of mouse retina and human tumor was dissected discarding lens, sclera and choroid, and harvested. Optic nerves, brains and BM were also harvested. Samples were snap-frozen in liquid nitrogen and stored at –80 °C until RNA extraction.

Tumor histology and immunohistochemistry (IHC)

After fixation, tissues were processed and embedded in paraffin using conventional automated systems. Four-micron sections were stained with conventional hematoxylin–eosin (H/E). Primary antibodies against retinoblastoma protein (pRB; NCL-L-RB-358) and synaptophysin (NCL-L-SYNAP-299) were from Leica BioSystems (Newcastle, UK), glial fibrillary acidic protein (GFAP) antibody (RP014) was from Diagnostic BioSystems (Pleasanton, CA) and nestin antibody (ABD69) was from Merck Millipore (Darmstadt, Germany). To stain human retinoblastoma cells in mouse tissues we used the human nuclei antibody (hNu; MAB4383, Merck Millipore).

RT-qPCR

Total RNA from retinoblastoma cells, pediatric glioma cells, neuroblastoma cells, engrafted retinoblastoma tumors, mouse retinas, brains, optic nerves and BM was isolated using TRIzol (Life Technologies). cDNA was synthetized with M-MLV reverse transcriptase system (Life Technologies) using 1 μg RNA. SuperScriptIII First-Strand Synthesis SuperMix (Life Technologies) was used to synthesize cDNA from CSF samples. Calibration curves were generated by serial dilutions of each cDNA from retinoblastoma cell models in cDNA from control (nontumor) mouse retinas, brains or BM. Expression of *GD2 synthase* and *CRX* mRNA was quantified in 10 μL reactions using SYBR® Green PCR Master Mix (Life Technologies) in a 7500 Sequence Detection System (Applied Biosystems, Foster City, CA). Sequences for *GD2 synthase* and *CRX* primers have been published elsewhere [21,26]. To analyze CRX mRNA expression using Taqman technology, the following primers and MGB probe were generated: Forward 5′-AGGTGGCTCTGAAGATCAATCTG-3′, reverse 5′-TTAGCCCTCCGGTTCTTGAA-3′, and probe 5′-FAM-CTGAGTCCAGGGTTC-3′-MGB.

Mouse tissues were used as negative controls. Relative expression of *GD2 synthase* or *CRX* mRNA was determined using the $2^{\Delta\Delta Ct}$ method [27]. TATA-box binding protein (TBP) mRNA was used as normalizing gene. Sequences for TBP transcript were forward 5′-GAACATCATGGATCAGAACAACAG-3′, reverse 5′-ATTGGTGTTCTGAATAGGCTGTG-3′, and probe for Taqman assays 5′-FAM-CTGCCACCTTACGCTCAGGGCTTGG-TAMRA-3′. Normalized values of relative *CRX* and *GD2 synthase* expression were represented as the percentage of human tumor cells in mouse tissues.

Kinetics of local tumor growth and extraocular dissemination

The *CRX* method was used to study the rate of local (intraocular) tumor growth and extraocular dissemination to the CNS and BM. By this method, human tumor load in specific mouse tissues was defined as the percentage of human tumor cells in mouse cells. A group of 20 mice was inoculated bilaterally with Y79 cells. At selected time points after inoculation (7, 14, 21, 28 days and endpoint) retinas (containing intraocular tumor), optic nerves, brains, BM and CSF were removed, snap-frozen and stored at –80 °C until RNA extraction and RT-qPCR analysis.

Statistics

Statistical analysis was performed with GraphPad Prism 5 software (La Jolla, CA). Aggregate data are presented as median values with standard deviation and median survivals were calculated using Kaplan–Meier curves.

Results

Establishment of primary retinoblastoma cultures with expression of GD2 and CRX

We established eight primary retinoblastoma cultures derived from six enucleated eyes. Clinical annotations of each tumor model including previous treatments are shown in Table 1. Five cultures were derived from RBT specimens and three were derived from RBVS. From Patients 1 and 8 we established primary cultures from both RBT and RBVS samples, while attempts to obtain stable cultures from RBVS samples from Patients 2 and 7 were unsuccessful. Enucleated eyes from Patients 3 and 5 presented only RBVS and RBT samples, respectively, available for culture. None of the patients received external beam radiotherapy prior to or after enucleation, nor developed metastatic retinoblastoma during follow up, and all are alive. Cultures grew as spheroids with high expression levels of ganglioside GD2 and the retinal progenitor marker CRX (Fig. 1A), confirming their tumorigenic origin.

The expression of *GD2 synthase* and *CRX* mRNA was quantified in the retinoblastoma cells and in one DIPG cell model, normalized to the expression of the Y79 retinoblastoma cell line (Fig. 1B). Normalized *GD2 synthase* expression was variable among the

Table 1
Clinical details of the patient-derived retinoblastoma cell models.

Patient	Germline RB1 mutation	Cell models	Tissue of origin	Age at diagnosis (months)	Age at enucleation (months)	Laterality	Chemotherapy
1	No	HSJD-RBT-1	Tumor	30	36	Unilateral	Yes[a]
		HSJD-RBVS-1	Vitreous				
2	Yes	HSJD-RBT-2	Tumor	7	13	Bilateral	Yes[b]
3	Yes	HSJD-RBVS-3	Vitreous	1	24	Bilateral	Yes[c]
5	No	HSJD-RBT-5	Tumor	7	24	Unilateral	Yes[d]
7	No	HSJD-RBT-7	Tumor	6	6	Unilateral	No
8	No	HSJD-RBT-8	Tumor	16	24	Unilateral	Yes[b]
		HSJD-RBVS-8	Vitreous				

[a] Four cycles of systemic carboplatin, etoposide and vincristine and one dose of topotecan and melphalan in the ophthalmic artery.
[b] Five doses of topotecan and melphalan in the ophthalmic artery.
[c] Six cycles of systemic carboplatin, etoposide and vincristine, two cycles of systemic cyclophosphamide, ruthenium brachytherapy, three cycles of systemic topotecan and one dose of topotecan and melphalan in the ophthalmic artery.
[d] Six cycles of systemic carboplatin, etoposide and vincristine, two doses of topotecan and melphalan in the ophthalmic artery, ruthenium brachytherapy.

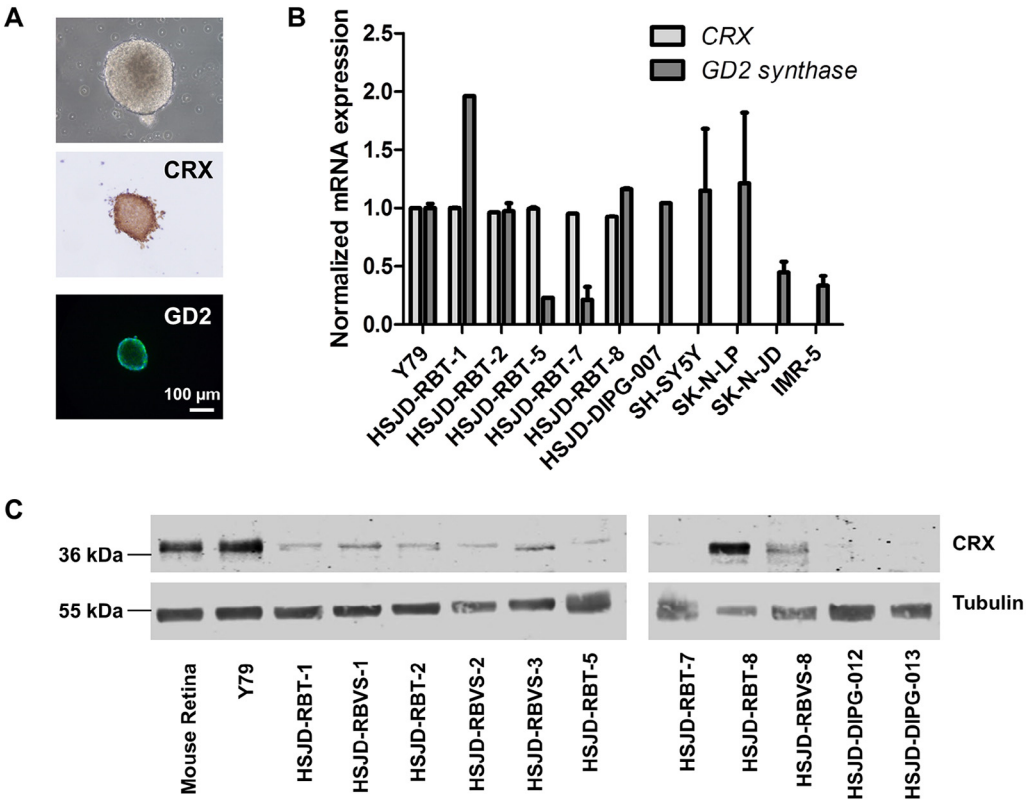

Fig. 1. Characterization of the primary retinoblastoma cultures. A) Retinoblastoma tumorspheres as observed in bright field microscopy (HSJD-RBVS-1), stained for the CRX transcription factor by IC (HSJD-RBT-1) and for GD2 ganglioside by IF (HSJD-RBVS-1). B) mRNA expression of *CRX* and *GD2 synthase* in the retinoblastoma models, in a DIPG model and in neuroblastoma cell lines (SYBR Green assay; transcript levels were quantified relative to those detected in Y79 cells; mean and standard deviation). *CRX* was not analyzed in neuroblastoma cell lines. C) CRX expression analyzed by western blot in mouse retina, Y79, retinoblastoma tumorspheres and two DIPG models.

retinoblastoma models (range 0.1–2.0), it was 1.0 in the DIPG model and in the range 0.3–1.2 for neuroblastoma cell lines. In contrast, the expression of *CRX* mRNA was uniform among the models (range 0.9–1.0) and it was not detected in the DIPG cell model.

Immunoblots showed positive CRX protein expression in tissues from retinal lineage (mouse retina and human retinoblastomas) but not in neuroectodermic tumors (two DIPG models) (Fig. 1C).

Chromosomal aberration profiles

We characterized overall genomic aberrations from two representative retinoblastoma tumors (Patients 2 and 8) and paired cultured tumor models (HSJD-RBT-2 and HSJD-RBT-8), through a whole-genome microarray analysis of DNA.

Patient 2 was heterozygous for the germline mutation c.1422-2A>G in *RB1*, related to predisposition to retinoblastoma [28]. Tumor from Patient 2 showed amplification (>10 copies) of the *MYCN* oncogene locus (2p24.3) (Fig. 2A). The amplicon included the full lengths of *MYCN*, *DDX1* and *FAM49A* genes, and part of the *NBAS* gene. However, other genes on chromosome 2p were affected by an amplification process (*LINC00299* (2p25.1) and *FAM84A* (2p24.3)). The paired cultured cells HSJD-RBT-2 conserved similar chromosomal alterations as compared to the original tumor, with additional changes including a chromosomal gain affecting 1q23.3-qter and LOH at 17p13.1-pter, and chromosome 2p amplified regions (Fig. 2B).

The chromosomal profile of tumor from Patient 8 showed gains and losses of large chromosomal regions (≥3 Mb) affecting chromosome arms 1q, 6p, 13q, 14q, 16q, 17q, 18p and Xq (Fig. 2C). Chromosome losses at 13q (13q14.2-q21.33) and 18p (18p11.21-p11.31) were associated with loss of heterozygosity. In addition, chromosome arm 13q showed a biallelic deletion (278 kbp) spanning the *RB1* locus (13q14). No gains and/or losses of whole chromosomes were observed. The chromosomal profile of the HSJD-RBT-8 cells was found to be almost identical to the primary tumor, with no significant additional changes (Fig. 2D).

Characterization of retinoblastoma xenografts

Upon intraocular inoculation, Y79 cells and four out of seven primary cultures engrafted in 100% of mouse eyes. Median survival times for eyes bearing Y79, HSJD-RBT-2, HSJD-RBT-5, HSJD-RBT-7 and HSJD-RBT-8 models were 31, 38, 45, 42 and 75 days, respectively (Fig. 3A), whereas models HSJD-RBT-1, HSJD-RBVS-1, HSJD-RBVS-3 did not engraft consistently (Fig. 3B). Representative tumor histology pictures are summarized in Fig. 4 for each tumor model (original biopsy and xenograft). Xenograft models HSJD-RBT-2, HSJD-RBT-5 and HSJD-RBT-8 recapitulated the presence of differentiated Homer Wright rosettes in the enucleated eyes of patients 2, 5 and 8. Tumor cells in HSJD-RBT-7 xenograft were undifferentiated, in accordance with the tumor histology of patient 7. Y79 showed undifferentiated tumor histology.

We found positive staining of synaptophysin and negative pRb expression in all xenografts and patient samples (Supplementary Fig. S1), confirming neuronal properties and loss of Rb protein by inactivation of the RB1 gene. Xenografts and patient samples also showed negative expression of GFAP and nestin, consistent with the retinal neuron origin of retinoblastoma [7,29].

At the endpoint all tumor models infiltrated retina, sub-retinal space, ciliary body, choroid and sclera (Fig. 5). Immunostaining with anti-human nuclei antibody (hNu) identified human cells invading mouse tissues. Large areas of tumor necrosis were observed in the Y79 model. Optic nerves were invaded by retinoblastoma cells in models HSJD-RBT-2, HSJD-RBT-8 and Y79. Brain dissemination was located in the subarachnoidal space for HSJD-RBT-2 and Y79 models. No tumor cells were identified in the brain parenchyma.

Molecular detection of human retinoblastoma cells in mouse tissues

To quantify the presence of retinoblastoma cells in mouse tissues, two different methods were performed. Initially, relative quantitation of *GD2 synthase* and *CRX* mRNA was conducted using SYBR green. cDNA from Y79 cells was used to build calibration curves for *GD2 synthase* and *CRX* mRNA in mouse retinas and brains (Fig. 6A). In this assay, the limit of detection (LOD) of *GD2 synthase* was equivalent to 1 retinoblastoma cell in 10^3 mouse brain cells and 1 cell in 10^4 mouse retinal cells. For *CRX*, the LOD was equivalent to 1 retinoblastoma cell in 10^4 mouse brain cells and 1 cell in 10^4 mouse retinal cells.

Because GD2 synthase showed limited sensitivity and poor linearity in the mouse brain (Fig. 6A), the *CRX* gene was selected for further refinement of the technique. To this end, a Taqman® assay was designed. Using this method the linearity of the calibration curves was improved and the LODs were reduced to 1 cell in 10^5 mouse brain cells and 1 cell in 10^4 mouse retinal cells (Fig. 6B). This assay provided 100% specificity and $1{:}10^5$ sensitivity.

Molecular (CRX) evaluation of local tumor growth rate and extraocular dissemination

Tumor (Y79) load in eyes, optic nerves and brains at days 7, 14, 21, 28 and endpoint is represented in Fig. 7. The maximum ocular load was achieved at day 28 (13.3 ± 3.0%). All optic nerves were infiltrated from day 21 onward and the level of infiltration increased until ocular endpoint. CNS dissemination was detected in 50% of animals at ocular endpoint. One CSF sample out of 12 mice was *CRX*-positive. *CRX* mRNA expression was consistently negative in BM samples.

Characterization of primary retinoblastoma xenografts by CRX *mRNA RT-qPCR*

Intraocular tumor burden, brain metastasis and BM invasion were evaluated at the ocular endpoint in orthotopic HSJD-RBT-2 and HSJD-RBT-5 models. Intraocular tumor load in mice bearing HSJD-RBT-2 tumors achieved a median value of 136% (±66%) and 4 out of 5 of mice showed positive CNS dissemination with a median CNS load of 0.0047% (±0.0845%) (Fig. 8). For the HSJD-RBT-5 model, local tumor burden represented 84.5% (±46.0%) of the intraocular content and no mice were positive for CNS dissemination (Fig. 8). The viability of the intraocular tumor tissue in both models at endpoint is shown in Fig. 9, as compared to the evident necrosis of the Y79 model. BM samples were *CRX*-negative in all mice.

Discussion

Here we have established new retinoblastoma models from patients that underwent enucleation after the failure of high local doses of chemotherapy agents [30] (Table 1). To immortalize cultures from patient biopsies we applied serum-free medium because the presence of serum can promote the growth and differentiation of cells that do not reproduce the original tumor genetics [31]. In contrast, the use of serum-free medium selects for highly tumorigenic cells that grow indefinitely as spheroids (or tumorspheres) and show positive expression of neuroendocrine markers (synaptophysin and MAP2), cancer stem cell markers Oct-4, nestin and Pax6 or, most importantly, negative expression of pRb, as the result of the *RB1* gene mutation or epigenetic inactivation [31,32]. Retinoblastoma spheroids cultured in serum-free medium engraft in mouse eyes [8,32]. However, it remained incompletely characterized whether the engrafted tumors from such cultures disseminate into the CNS.

One of the goals of our work was to characterize the metastatic properties of the new cell models grown in serum-free

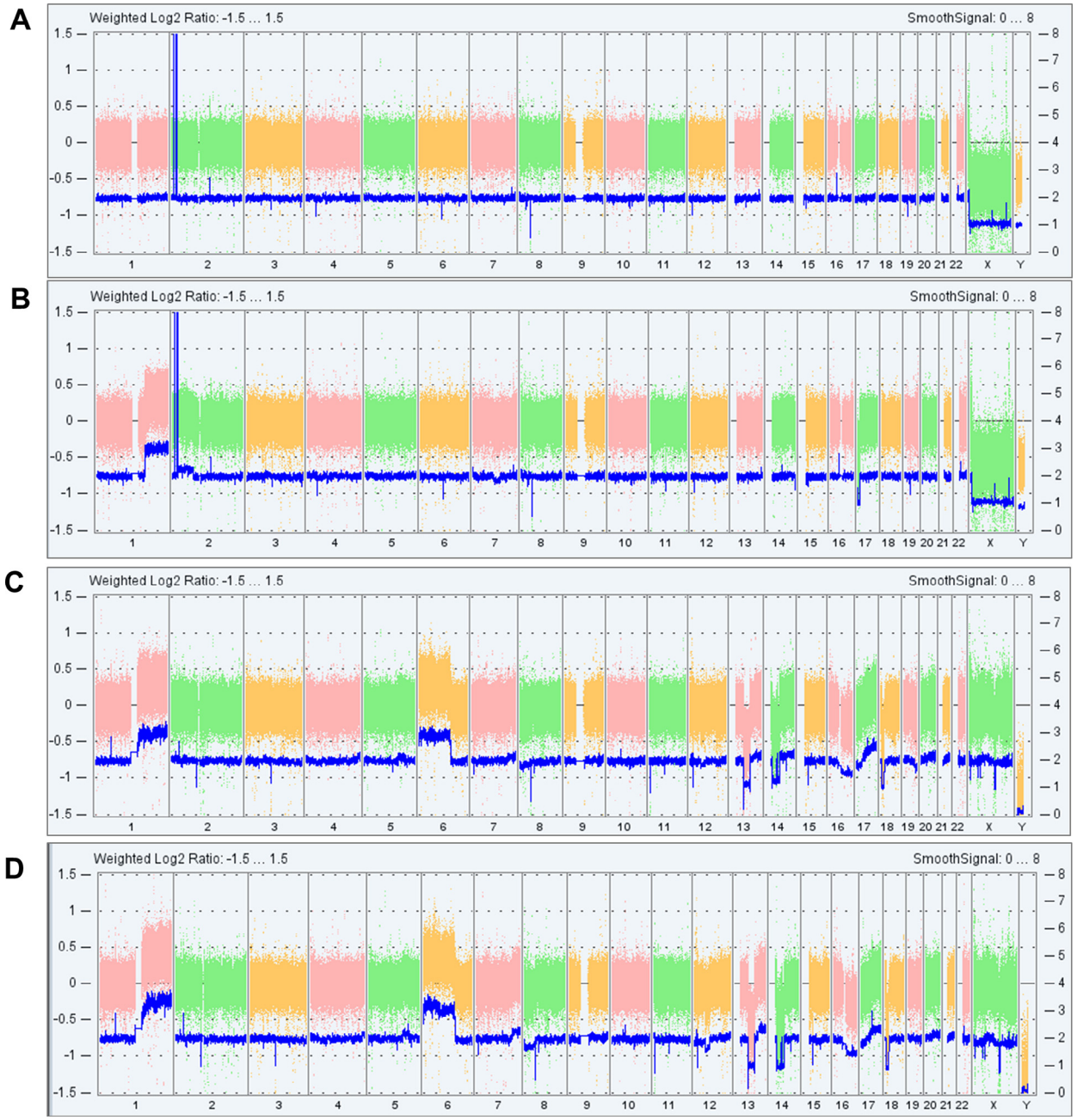

Fig. 2. Chromosomal microarrays of paired tumors and xenografts. Whole genome visualization of the chromosomal profiles of RBT biopsies from Patient 2 (A) and Patient 8 (C) and of the matched cultured tumor models HSJD-RBT-2 at passage 7 (B) and HSJD-RBT-8 at passage 3 (D). The $\log_2$ copy number track and the smooth signal indicate the segmental and high copy number (amplification) aberrations observed in the samples. Each column represents a different chromosome.

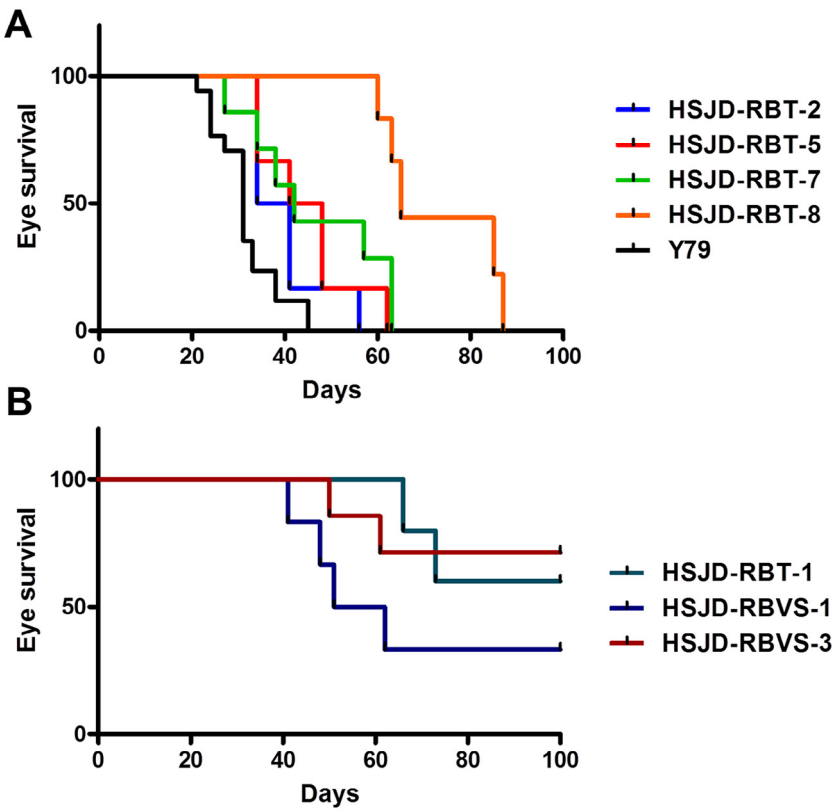

Fig. 3. Eye survival curves of retinoblastoma xenografts. A) Survival curves of models with 100% engraftment rate, including reference model Y79. B) Survival curves of models with erratic engraftment.

medium. First we evaluated the capability of each retinoblastoma primary culture to form tumors after intraocular injection and found a high engraftment rate among the models. Several genetic and histological features of the original patient biopsies were recapitulated by the new xenografts (Figs. 2 and 4 and Supplementary Fig. S1). The human cell staining helped detect the retinoblastoma kinetics of invasion at the single-cell level and we could observe infiltration in the meningeal space of mice bearing HSJD-RBT-2 tumors (Fig. 5) confirming the metastatic properties of this model. In previous studies using the cell line Y79, CNS metastases were evaluated by conventional histology because Y79 cells invade extensively the CNS [12,33]. However, in tumor models derived from primary cultures, such as the ones we report here, CNS infiltration could have been underestimated by conventional histopathology evaluation or even by the hNu IHC method. Thus, we considered using gene markers to detect retinoblastoma CNS metastases. Human gene detection in xenografts has already been proposed as a tool to evaluate tumor progression and dissemination. For instance, a real time PCR method was developed to study the ability of neuroblastoma cells to colonize the mouse BM after orthotopic inoculation in the adrenal gland [34].

In our study we evaluated *GD2 synthase* and *CRX* as suitable MDD markers, based on previous clinical studies by Laurent et al. and Torbidoni et al., associating *GD2 synthase* and *CRX* mRNA levels with extraocular disease in patients with retinoblastoma [20,21]. The *GD2 synthase* method is simple, although endogenous GD2 expression of nontumor cells can interfere with the results [16]. Our experimental results confirmed such interference and led us to select CRX

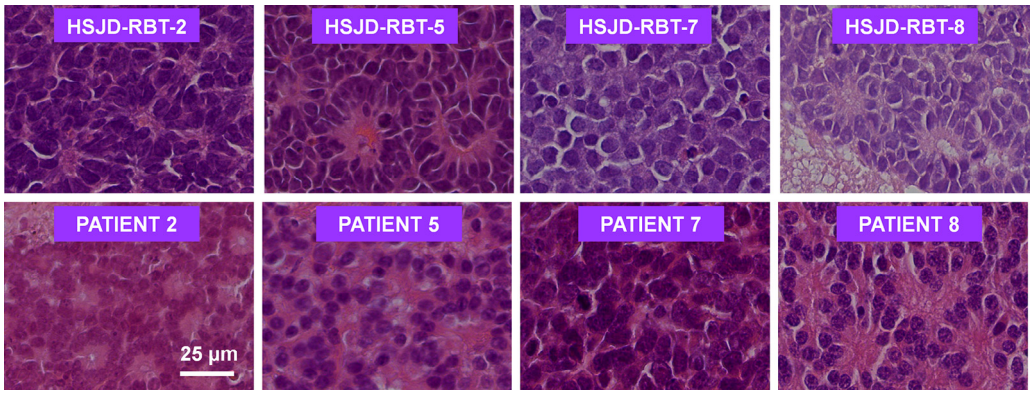

Fig. 4. Comparative histology of original human retinoblastoma biopsies and counterpart xenografts. Note the absence of rosettes in model HSJD-RBT-7 and patient 7 tumor. The images were obtained using a microscope with a 40× objective.

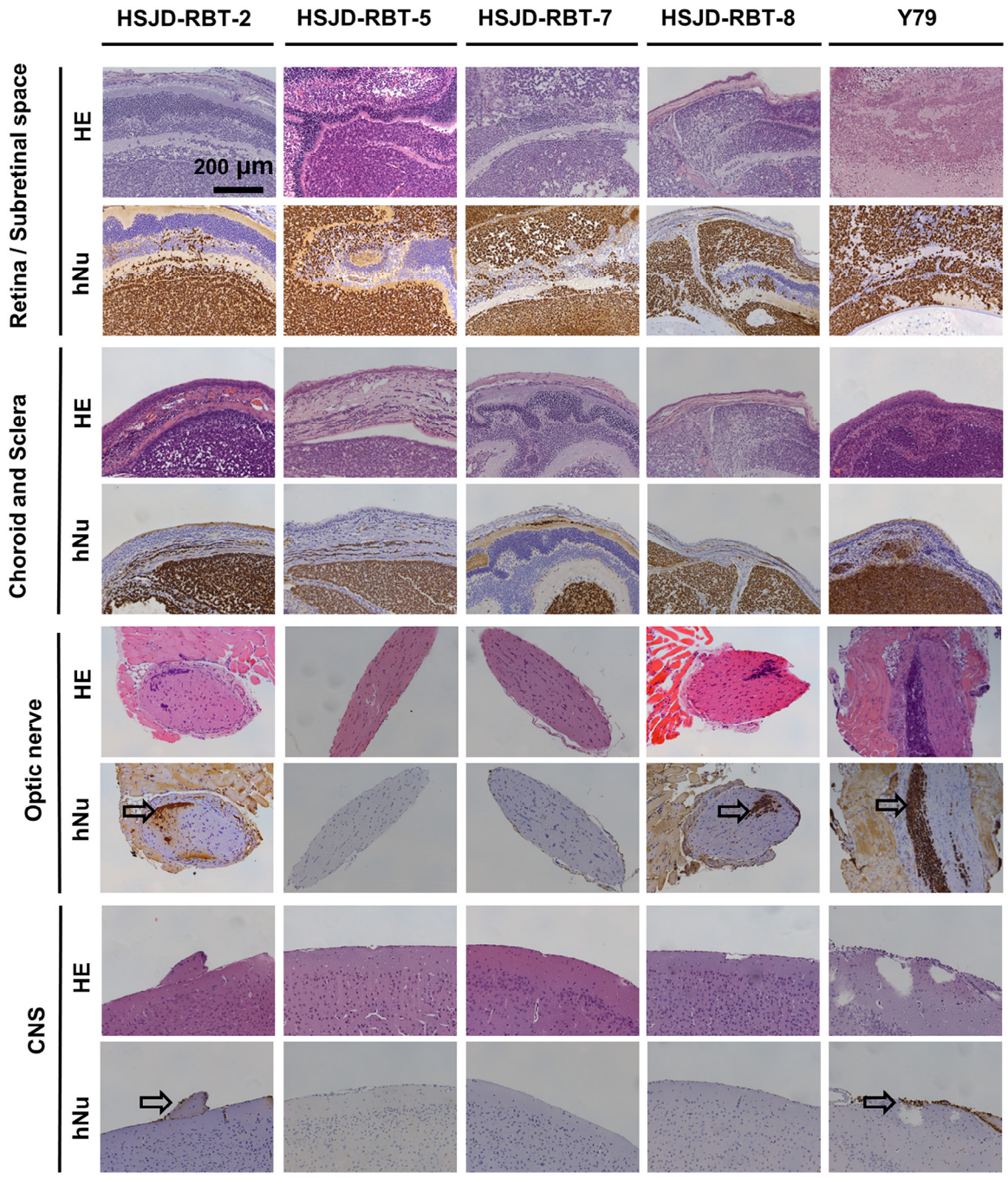

Fig. 5. Histology and invasion of human retinoblastoma xenografts. Histology was evaluated by H-E and hNu staining. Human retinoblastoma cells are present in the vitreous, retina, subretinal space, choroid, sclera, optic nerve and brain (subarachnoidal space) depending on the tumor model. Arrows: human cells (brown nuclei) invading optic nerve and brain meninges. The images were obtained using a microscope with a 20× objective. (For interpretation of the references to color in this figure legend, the reader is referred to the web version of this article.)

for *in vivo* studies. Even though immunoblotting detected CRX protein expressed by the mouse retina (Fig. 1C), our Taqman analysis was selective enough to discern between mouse and human *CRX* mRNA, so that no negative control tissues expressed our *CRX* transcript by RT-qPCR.

To set up the technique *in vivo* and to study the kinetics of tumor growth and CNS dissemination we used Y79 cells, a well-known cell model of retinoblastoma [12]. In this model we found that the intraocular tumor burden was greater at 28 days post-tumor inoculation than at endpoint (Fig. 7). This could be explained by the vast tumor necrosis produced in the posterior segment of the eye in the Y79 xenografts. Necrosis could also explain the differences in viable tumor load at endpoint between the Y79 (10% viable tumor load) and the primary models (both 100% tumor load) (Figs. 7–9). Because our method quantifies only viable retinoblastoma cells, it could be useful to detect treatment-induced tumor necrosis in future preclinical studies.

The quantitative potential of the *CRX* method, showing progressive infiltration of the optic nerve over time, provides insight into the mechanism of retinoblastoma xenograft dissemination to CNS. Our results using Y79 xenografts suggest that cells spread from the retina to the optic nerve progressively during tumor development,

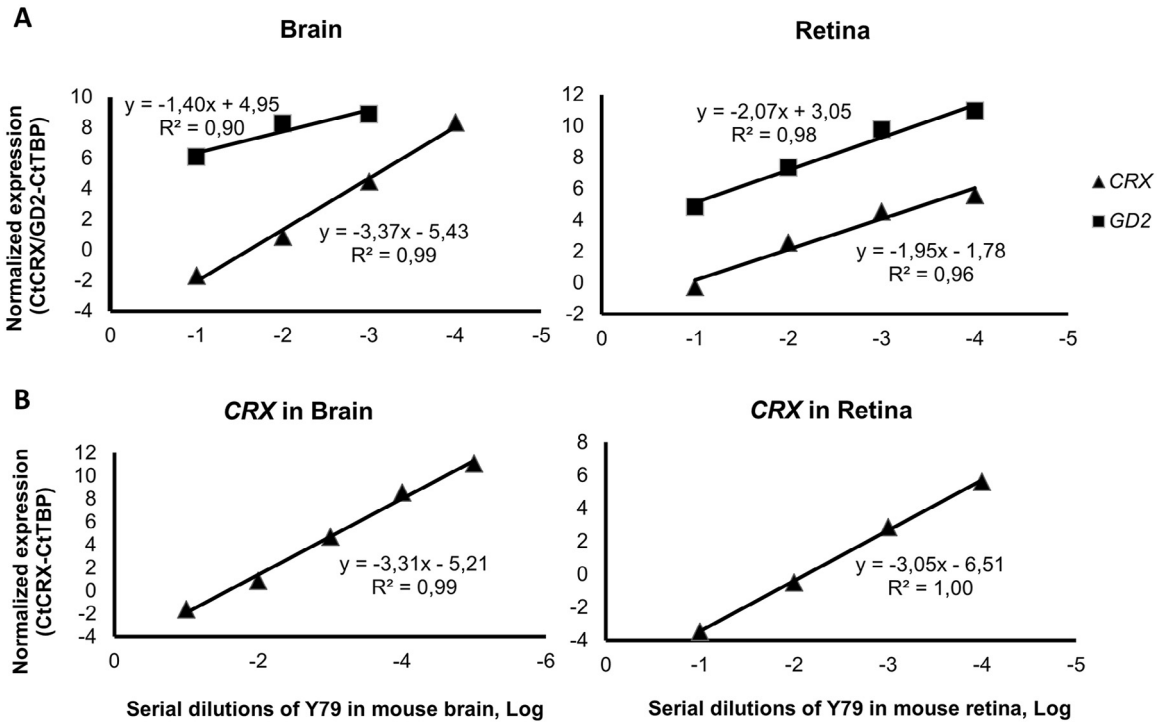

Fig. 6. Limit of detection of *GD2 synthase* and *CRX* mRNA expression in mouse tissues. A) *CRX* and *GD2 synthase* limit of detection in mouse brain and retina using SYBR Green. B) *CRX* limit of detection in mouse brain and retina using Taqman.

as observed in zebrafish models at single-cell level [35]. Only when intraocular tumors reached advanced stages (28 days and endpoint) CNS dissemination was detected in a high percentage of mice (54%). All mice developing CNS metastases presented optic nerve CRX positivity. These results, together with the hNu staining in the brain meninges of models Y79 and HSJD-RBT-2, support a pathway of dissemination in which tumor cells travel through the optic nerve and its sheath into the circulating subarachnoid fluid to reach the spinal cord and distant sites of the CNS [13]. We detected one positive CSF sample in a CRX-positive brain of one Y79 xenograft, recapitulating the clinical scenario of a brain metastatic retinoblastoma in the preclinical setting. Nevertheless, we did not detect CSF dissemination in any other mice with CNS involvement, probably due to the small samples (10 µL CSF collected from the cisterna magna). Of note, the lack of positive *CRX* expression in the BM of all the models suggests that they do not follow the hematogenous route of dissemination, as reported in patients with metastatic retinoblastoma [21].

Further studies should be carried out to understand why the new xenografts show diverse patterns of CNS dissemination. Whether extraocular metastasis of retinoblastoma is promoted by specific phenotypic properties of the tumor remains not totally understood, although recent studies provide candidate molecules, such as long noncoding RNAs, significantly associated to choroidal and optic nerve invasion, and patient survival [36].

In summary, we present a novel set of retinoblastoma xenografts and propose an objective and sensitive molecular method (*CRX* RT-qPCR detection) to quantify the local and metastatic tumor burden of these models. This method proved useful also to characterize the pathway of dissemination of the tumor cells from the ocular tissues and to discern between viable and necrotic cells. The method is currently used in our laboratory to evaluate more accurately the activity

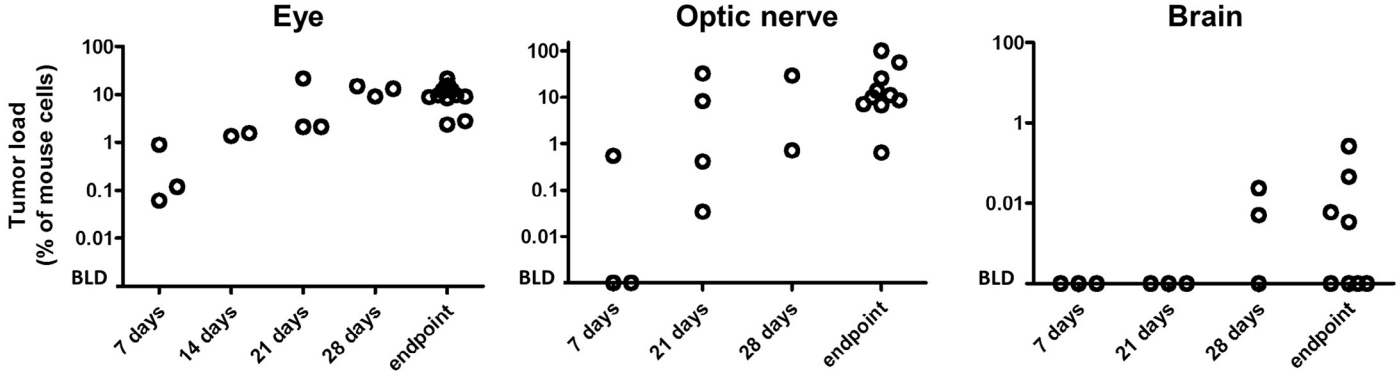

Fig. 7. Local tumor growth and extraocular dissemination kinetics of Y79 xenografts. Values of retinoblastoma tumor burden in intraocular content, optic nerve and brain were measured by *CRX* expression at 7, 14, 21 and 28 days and at endpoint in mice bearing orthotopic Y79 tumors. Each dot represents the tumor load in an individual eye, optic nerve or brain. BLD: below limit of detection.

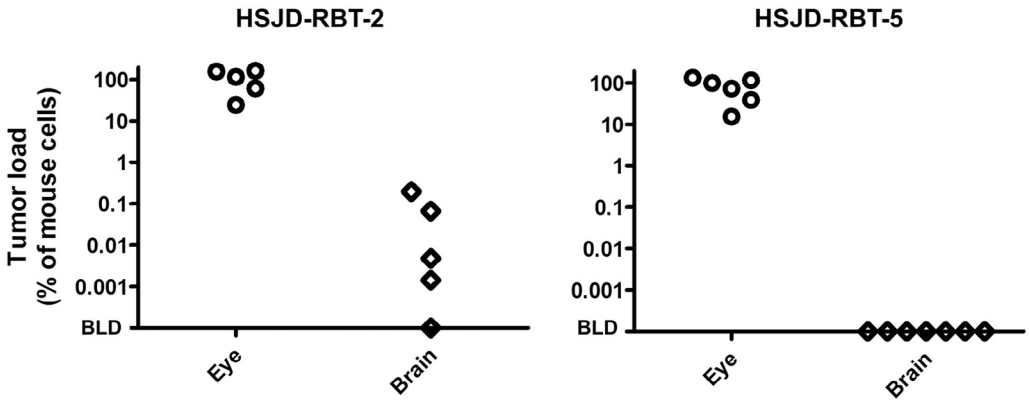

Fig. 8. Local (ocular) tumor burden and brain metastasis in primary retinoblastoma xenografts at ocular endpoint, as determined by the *CRX* method. Each dot represents the tumor load in an individual eye or brain. BLD: below limit of detection.

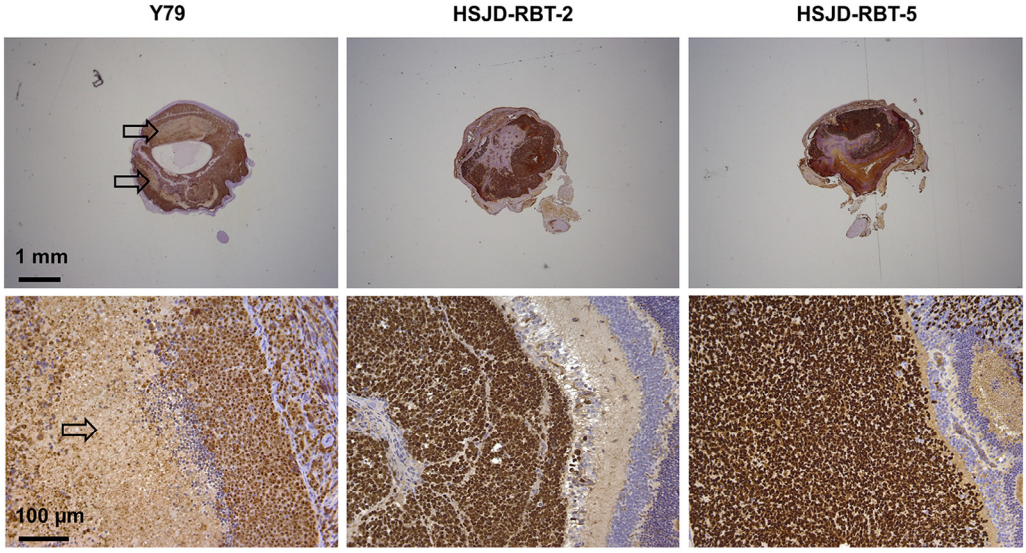

Fig. 9. Extensive tumor necrosis in intraocular retinoblastoma (hNu staining). Note necrosis in the Y79 model (arrows). Mouse nuclei are counterstained with hematoxylin. The images were obtained using a microscope with 2× (top pictures) or 20× objectives.

of innovative therapies against retinoblastoma to control local tumor growth and to prevent CNS dissemination.

Acknowledgements

AMC acknowledges funding from ISCIII-FEDER (CP13/00189), the AECC Scientific Foundation (AIO 2010), European Union Seventh Framework Programme (FP7/2007–2013) under Marie Curie International Reintegration Grant (PIRG-08-GA-2010-276998) and Retos MINECO (Cure4RB project RTC-2015-4319-1). We thank Isadora Lemos for performing DNA extractions. This work was supported by the Xarxa de Bancs de Tumors de Catalunya (XBTC) sponsored by Pla Director d'Oncologia de Catalunya.

Conflict of interest

The authors declare no conflict of interest.

Appendix: Supplementary material

Supplementary data to this article can be found online at doi:10.1016/j.canlet.2016.06.012.

References

[1] D.H. Abramson, Retinoblastoma: saving life with vision, Annu. Rev. Med. 65 (2014) 171–184.
[2] D.H. Abramson, C.L. Shields, F.L. Munier, G.L. Chantada, Treatment of retinoblastoma in 2015: agreement and disagreement, JAMA Ophthalmol. 133 (2015) 1341–1347.
[3] Y.P. Gobin, I.J. Dunkel, B.P. Marr, S.E. Brodie, D.H. Abramson, Intra-arterial chemotherapy for the management of retinoblastoma: four-year experience, Arch. Ophthalmol. 129 (2011) 732–737.
[4] J.H. Francis, D.H. Abramson, M.C. Gaillard, B.P. Marr, M. Beck-Popovic, F.L. Munier, The classification of vitreous seeds in retinoblastoma and response to intravitreal melphalan, Ophthalmology 122 (2015) 1173–1179.
[5] G.L. Chantada, I.J. Dunkel, C.B. Antoneli, M.T. de Davila, V. Arias, K. Beaverson, et al., Risk factors for extraocular relapse following enucleation after failure of chemoreduction in retinoblastoma, Pediatr. Blood Cancer 49 (2007) 256–260.
[6] J. McEvoy, J. Flores-Otero, J. Zhang, K. Nemeth, R. Brennan, C. Bradley, et al., Coexpression of normally incompatible developmental pathways in retinoblastoma genesis, Cancer Cell 20 (2011) 260–275.
[7] X.L. Xu, Y. Fang, T.C. Lee, D. Forrest, C. Gregory-Evans, D. Almeida, et al., Retinoblastoma has properties of a cone precursor tumor and depends upon cone-specific MDM2 signaling, Cell 137 (2009) 1018–1031.
[8] W.S. Bond, L. Wadhwa, L. Perlaky, R.L. Penland, M.Y. Hurwitz, R.L. Hurwitz, et al., Establishment and propagation of human retinoblastoma tumors in immune deficient mice, J. Vis. Exp. 54 (2011) 2644.
[9] R.C. Brennan, S. Federico, C. Bradley, J. Zhang, J. Flores-Otero, M. Wilson, et al., Targeting the p53 pathway in retinoblastoma with subconjunctival Nutlin-3a, Cancer Res. 71 (2011) 4205–4213.

[10] N.A. Laurie, J.K. Gray, J. Zhang, M. Leggas, M. Relling, M. Egorin, et al., Topotecan combination chemotherapy in two new rodent models of retinoblastoma, Clin. Cancer Res. 11 (2005) 7569–7578.
[11] K.M. Nemeth, S. Federico, A.M. Carcaboso, Y. Shen, P. Schaiquevich, J. Zhang, et al., Subconjunctival carboplatin and systemic topotecan treatment in preclinical models of retinoblastoma, Cancer 117 (2011) 421–434.
[12] P. Chevez-Barrios, M.Y. Hurwitz, K. Louie, K.T. Marcus, V.N. Holcombe, P. Schafer, et al., Metastatic and nonmetastatic models of retinoblastoma, Am. J. Pathol. 157 (2000) 1405–1412.
[13] C.J. Mackay, D.H. Abramson, R.M. Ellsworth, Metastatic patterns of retinoblastoma, Arch. Ophthalmol. 102 (1984) 391–396.
[14] S. Zacharoulis, D.H. Abramson, I.J. Dunkel, More aggressive bone marrow screening in retinoblastoma patients is not indicated: the memorial Sloan-Kettering cancer center experience, Pediatr. Blood Cancer 46 (2006) 56–61.
[15] M.S. Lo Piccolo, N.K. Cheung, I.Y. Cheung, GD2 synthase: a new molecular marker for detecting neuroblastoma, Cancer 92 (2001) 924–931.
[16] M. Suzuki, N.K. Cheung, Disialoganglioside GD2 as a therapeutic target for human diseases, Expert Opin. Ther. Targets 19 (2015) 349–362.
[17] T. Furukawa, E.M. Morrow, C.L. Cepko, Crx, a novel otx-like homeobox gene, shows photoreceptor-specific expression and regulates photoreceptor differentiation, Cell 91 (1997) 531–541.
[18] D.D. Glubrecht, J.H. Kim, L. Russell, J.S. Bamforth, R. Godbout, Differential CRX and OTX2 expression in human retina and retinoblastoma, J. Neurochem. 111 (2009) 250–263.
[19] G.L. Chantada, J. Rossi, F. Casco, A. Fandino, M. Scopinaro, M.T. de Davila, et al., An aggressive bone marrow evaluation including immunocytology with GD2 for advanced retinoblastoma, J. Pediatr. Hematol. Oncol 28 (2006) 369–373.
[20] V.E. Laurent, C. Sampor, V. Solernou, J. Rossi, M. Gabri, S. Eandi-Eberle, et al., Detection of minimally disseminated disease in the cerebrospinal fluid of children with high-risk retinoblastoma by reverse transcriptase-polymerase chain reaction for GD2 synthase mRNA, Eur. J. Cancer 49 (2013) 2892–2899.
[21] A.V. Torbidoni, V.E. Laurent, C. Sampor, D. Ottaviani, V. Vazquez, M.R. Gabri, et al., Association of cone-rod homeobox transcription factor messenger RNA with pediatric metastatic retinoblastoma, JAMA Ophthalmol. 133 (2015) 805–812.
[22] M. Monje, S.S. Mitra, M.E. Freret, T.B. Raveh, J. Kim, M. Masek, et al., Hedgehog-responsive candidate cell of origin for diffuse intrinsic pontine glioma, Proc. Natl. Acad. Sci. U.S.A. 108 (2011) 4453–4458.
[23] K.R. Taylor, A. Mackay, N. Truffaux, Y.S. Butterfield, O. Morozova, C. Philippe, et al., Recurrent activating ACVR1 mutations in diffuse intrinsic pontine glioma, Nat. Genet. 46 (2014) 457–461.
[24] C. Kilkenny, W.J. Browne, I.C. Cuthill, M. Emerson, D.G. Altman, Improving bioscience research reporting: the ARRIVE guidelines for reporting animal research, J. Pharmacol. Pharmacother. 1 (2010) 94–99.
[25] L. Liu, K. Duff, A technique for serial collection of cerebrospinal fluid from the cisterna magna in mouse, J. Vis. Exp. 21 (2008) 960.
[26] I.Y. Cheung, N.K. Cheung, Quantitation of marrow disease in neuroblastoma by real-time reverse transcription-PCR, Clin. Cancer Res. 7 (2001) 1698–1705.
[27] K.J. Livak, T.D. Schmittgen, Analysis of relative gene expression data using real-time quantitative PCR and the 2(-Delta Delta C(T)) Method, Methods 25 (2001) 402–408.
[28] M. Taylor, C. Dehainault, L. Desjardins, F. Doz, C. Levy, X. Sastre, et al., Genotype-phenotype correlations in hereditary familial retinoblastoma, Hum. Mutat. 28 (2007) 284–293.
[29] X.L. Xu, H.P. Singh, L. Wang, D.L. Qi, B.K. Poulos, D.H. Abramson, et al., Rb suppresses human cone-precursor-derived retinoblastoma tumours, Nature 514 (2014) 385–388.
[30] A. Parareda, J. Catala, A.M. Carcaboso, T. Sola, O. Cruz, J. Diaz, et al., Intra-arterial chemotherapy for retinoblastoma. Challenges of a prospective study, Acta Ophthalmol. 92 (2014) 209–215.
[31] W.S. Bond, P.Y. Akinfenwa, L. Perlaky, M.Y. Hurwitz, R.L. Hurwitz, P. Chevez-Barrios, Tumorspheres but not adherent cells derived from retinoblastoma tumors are of malignant origin, PLoS ONE 8 (2013) e63519.
[32] B. Ma, X. Lei, Y. Guan, L.S. Mou, Y.F. Yuan, H. Yue, et al., Maintenance of retinal cancer stem cell-like properties through long-term serum-free culture from human retinoblastoma, Oncol. Rep. 26 (2011) 135–143.
[33] L. Wadhwa, M.Y. Hurwitz, P. Chevez-Barrios, R.L. Hurwitz, Treatment of invasive retinoblastoma in a murine model using an oncolytic picornavirus, Cancer Res. 67 (2007) 10653–10656.
[34] L. Edry Botzer, S. Maman, O. Sagi-Assif, T. Meshel, I. Nevo, T. Bauerle, et al., Lung-residing metastatic and dormant neuroblastoma cells, Am. J. Pathol. 179 (2011) 524–536.
[35] X. Chen, J. Wang, Z. Cao, K. Hosaka, L. Jensen, H. Yang, et al., Invasiveness and metastasis of retinoblastoma in an orthotopic zebrafish tumor model, Sci. Rep. 5 (2015) 10351.
[36] S. Su, J. Gao, T. Wang, J. Wang, H. Li, Z. Wang, Long non-coding RNA BANCR regulates growth and metastasis and is associated with poor prognosis in retinoblastoma, Tumour Biol. 36 (2015) 7205–7211.